Polaronic effects on the resistivity of manganite thin films

Michael Ziese and Chatchai Srinitiwarawong
Department of Physics, University of Sheffield, Sheffield S3 7RH, United Kingdom
(Received 15 April 1998; revised manuscript received 17 June 1998)

The high-temperature resistivity of $La_{0.7}Ca_{0.3}MnO_3$ and $La_{0.7}Ba_{0.3}MnO_3$ thin films on various substrates $LaAlO_3$, $SrTiO_3$, and Si was investigated. We show that the intrinsic resistivity of high-quality epitaxial films in the paramagnetic phase has a thermally activated form, whereas the extrinsic resistivity found in polycrystalline films follows a variable range hopping law. The small activation energies measured are not compatible with the formation of a band gap; instead they indicate polaron hopping. The polaron mobility is drastically enhanced by the ferromagnetic ordering. We show that the reduction of the polaron activation energy below the Curie temperature is linear in the magnetization. The shift of the metal-insulator transition temperature depends sublinearly on the applied field. [S0163-1829(98)02841-0]

I. INTRODUCTION

The magnetic perovskites of the type $La_{(1-x)}A_xMnO_3$ have attracted considerable research activity lately. A stands for a divalent atom: $A=$Ca, Sr, Ba, Pb. At the doping level $x=0.3$ these compounds are ferromagnets with a Curie temperature near room temperature. The transition to magnetism is accompanied by a metal-insulator transition, the manganites being nonmetallic above and metallic below the Curie temperature. The metal-insulator transition strongly depends on the applied magnetic field, thus leading to a large ''colossal'' magnetoresistance near the transition temperature.[1]

The nature of the high-temperature phase of the manganites is controversial. Resistivity measurements mostly show a negative slope of the resistivity above the Curie temperature. No consensus, however, has been reached over the exact temperature dependence and the relevant models. At present three models are discussed,[1] i.e., a band-gap model, a variable-range hopping model, and a nearest-neighbor hopping model for the transport of small polarons. These models will be briefly discussed in Sec. II. Some experimental support can be found in the literature for each model.[2–4] Since the properties of the manganites depend strongly on the microstructure and the oxygen content, investigations on various thin films of different quality have been performed. However, a detailed, comparative study that separates intrinsic and extrinsic effects has not emerged.

In this work we investigate the high-temperature phase of the manganites using resistivity measurements in the range $70<T<600$ K. We present measurements on $La_{0.7}Ca_{0.3}MnO_3$ and $La_{0.7}Ba_{0.3}MnO_3$ films of different quality, i.e., annealed and as-deposited films on $LaAlO_3$, annealed films on $SrTiO_3$, as well as annealed and as-deposited films on Si.

The data clearly show that the high-temperature resistivity of the epitaxial films on $LaAlO_3$ and $SrTiO_3$ has a thermally activated form. The values of the activation energies are in favor of a model for small-polaron hopping in the adiabatic limit. On the other hand, the polycrystalline films on Si follow nicely the variable-range hopping (VRH) model. These findings clearly show that the VRH model describes extrinsic behavior found in low-quality films. We experimentally find that the activation energy for polaron hopping is reduced in the ferromagnetic phase by a term linear in the magnetization. The metal-insulator transition shifts with the applied field sublinearly to higher temperatures.

II. THEORETICAL MODELS

It is well accepted that the mechanism of double exchange between Mn^{3+} and Mn^{4+} ions is essential to understand the magnetic and transport properties of the manganites.[5,6] In this model electrons hopping from Mn^{3+} to Mn^{4+} ions experience a strong on-site Hund's-rule coupling J_H that leads to an effective hopping integral of the form $t=t_0\cos(\theta/2)$. In a classical treatment θ is the angle between the manganese core spins. First calculations of the resistivity in the relevant limit $J_H \gg t$ were performed by Searle and Wang[7] and Kubo and Ohata[8] in a mean-field model. In those calculations an essentially temperature-independent resistivity above T_C was obtained.

Recent models by Millis *et al.*[9] and Röder *et al.*[10] included spin correlations and the effects of a strong electron-phonon coupling due to the dynamic Jahn-Teller effect and obtained results in qualitative agreement with experiment. The resistivity above T_C strongly depends on the electron-phonon-coupling strength and can be tuned from semiconducting to metallic behavior.[9] Röder *et al.* found the formation of small magnetopolarons above T_C that become ''self-trapped.''[10]

All these models neglect carrier localization by random charge fluctuations or random fluctuations in the magnetic potential due to the doping atoms. Localization phenomena are thought to be important since the conduction band is relatively narrow with a width of about 1 eV.[1] Especially Coey and co-workers[3,11] proposed a model of carrier localization by random fluctuations in the Hund's-rule coupling. Localization might lead to the formation of a mobility edge or to variable-range hopping between the localized states.

At present three models are used to fit high-temperature resistivity data on the manganites, i.e., a simple Arrhenius law,[2] a polaron model,[4] and a variable-range hopping model.[3] We discuss these here briefly.

(1) An Arrhenius law

TABLE I. Parameters of the various samples investigated in this work. T_C denotes the Curie temperature derived from the magnetization and T_r denotes the temperature of maximum positive zero-field resistivity slope.

Sample	Substrate	Heat treatment	T_C (K)	T_r (K)
LCA1SR	$SrTiO_3$	Annealed	275.2	275.0
LCA1LA	$LaAlO_3$	Annealed	272.5	271.3
LCD1LA	$LaAlO_3$	As-deposited	224.6	233.7
LCD2LA	$LaAlO_3$	As-deposited		228.3
LCD3LA	$LaAlO_3$	As-deposited	228.8	229.1
LCA1SI	Si	Annealed	259.9	104
LCD1SI	Si	As-deposited	230.5	150
LBA1LA	$LaAlO_3$	Annealed	313.3	312.8
LBD1LA	$LaAlO_3$	As-deposited	297.5	294.8
LBD1SI	Si	As-deposited	301.7	98
LBA1SR	$SrTiO_3$	Annealed	276	135

$$\rho=\rho_\infty \exp\left[\frac{E_g}{2kT}\right] \tag{1}$$

is generally used to model activated behavior due to a band gap E_g or a mobility edge. However, it has to be kept in mind that a pure Arrhenius law might be a very crude approximation. In fact, the resistivity $\rho=1/(ne\mu)$ might display a temperature-dependent prefactor due to the carrier mobility μ or the carrier density n. Though the carrier concentration is dominated by the thermally activated form, it might nevertheless display a temperature-dependent prefactor determined by the particular density of states. In semiconductors it is sometimes found that the temperature dependences of the mobility and the carrier-density prefactor cancel.

(2) Nearest-neighbor hopping of small polarons (Holstein polarons) leads to a mobility with thermally activated form. In the adiabatic regime the charge-carrier motion is faster than the lattice vibrations and the drift mobility is given by

$$\mu=\frac{3ea^2}{2}\frac{\omega_0}{2\pi kT}\exp\left[-\frac{W_p}{kT}\right] \tag{2}$$

with $W_p=E_p/2-t$. E_p denotes the polaron formation energy, t the electronic transfer integral, ω_0 the longitudinal optical-phonon frequency, a the hopping distance, and e the electronic charge. Equation (2) is valid for temperatures larger than half the Debye temperature Θ_D. This is fulfilled for the samples considered here, which have a Curie temperature $T_C>\Theta_D/2\sim 150-200$ K.[12]

In the nonadiabatic limit the charge-carrier's motion is slow compared to the lattice vibrations and the drift mobility is given by

$$\mu=\frac{3ea^2}{2\hbar}\frac{t^2}{kT}\left(\frac{\pi}{4W_pkT}\right)^{1/2}\exp\left[-\frac{W_p}{kT}\right] \tag{3}$$

with $W_p=E_p/2$. The nonadiabatic limit is applicable if

$$t\ll t_{\max}=\left(\frac{2W_pkT}{\pi}\right)^{1/4}\left(\frac{\hbar\omega_0}{\pi}\right)^{1/2}. \tag{4}$$

The resistivity is obtained from $\rho=1/(ne\mu)$.

(3) If the carriers are localized by random potential fluctuations, Mott's variable-range hopping expression[13]

$$\rho=\rho_\infty \exp\left[\left(\frac{T_0}{T}\right)^{1/4}\right] \tag{5}$$

is appropriate to describe the experimental data. The temperature scale T_0 is related to the localization length ξ by[13]

$$kT_0=\frac{24}{\pi N(E_F)\xi^3}. \tag{6}$$

$N(E_F)$ denotes the density of states at the Fermi level.

III. EXPERIMENTAL DETAILS

$La_{0.7}Ca_{0.3}MnO_3$ (LCMO) and $La_{0.7}Ba_{0.3}MnO_3$ (LBMO) thin films have been deposited on $LaAlO_3$ (001), $SrTiO_3$ (001), and Si (001) substrates using pulsed laser deposition. A XeCl Excimer laser (308 nm, Lambda Physik) with a fluence near the ablation threshold is used to ablate from a stoichiometric ceramic target onto the heated substrate. With the exception of sample LBA1SR the substrate temperatures were about 650 °C and about 700 °C for the deposition of the LCMO and the LBMO films, respectively. The sample numbering scheme is the following: LC/LB stands for $La_{0.7}Ca_{0.3}MnO_3$ or $La_{0.7}Ba_{0.3}MnO_3$, D/A stands for as-deposited/annealed, and LA,SP,S1 refer to the substrate. The oxygen partial pressure was kept constant during ablation at 100 m Torr. The LBMO film LBA1SR was deposited under the same conditions as the LCMO films. The as-deposited film was insulating. Some of the films were postannealed for 2 h at 950 °C in flowing oxygen. LCMO and LBMO films with a thickness of about 100 nm have been fabricated. As-deposited and postannealed films and films deposited on different substrates ($LaAlO_3$, $SrTiO_3$, and Si) are compared. The substrate material, postdeposition treatment, Curie temperature T_C and temperature of maximum zero-field resistivity slope T_r are given in Table I.

Resistivity measurements were performed in a continuous-flow cryostat (Oxford Instruments) using a standard four-point configuration. A constant current in the range between 10 μA and 1 mA was supplied by a home-made

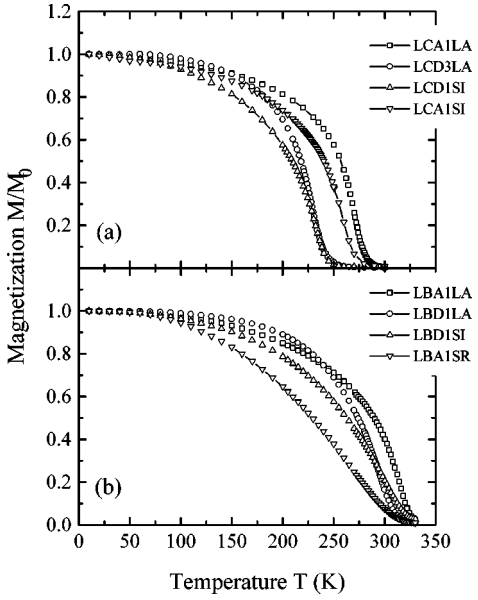

FIG. 1. The magnetization of various (a) LCMO and (b) LBMO films with a thickness of about 100 nm. The magnetization was measured in a field of 1 kG applied parallel to the film.

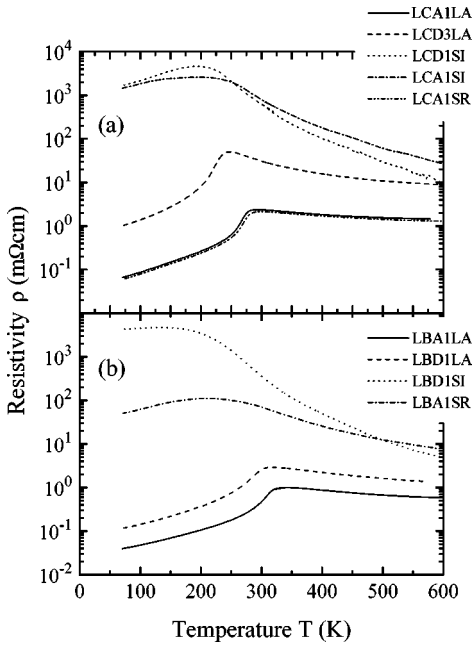

FIG. 2. Zero-field resistivity of various (a) LCMO and (b) LBMO films with a thickness of about 100 nm on different substrates.

current source and the voltage across the sample was measured with a nanovoltmeter (Keithley model 182). The high-temperature measurements were performed in an insulated glass tube in air. Contacts were made with silver paste for the low-temperature measurements and with silver paste or mechanical clamping for the high-temperature measurements. A van der Pauw configuration was always used.[14] The magnetic field was oriented in the film plane.

Magnetization measurements were performed in a superconductor quantum interference device magnetometer (MPMS-5, Quantum Design). The magnetic field was always oriented parallel to the film.

IV. RESULTS

A. Ferromagnetic and metal-insulator transition

Magnetization measurements in an applied field of 1 kG parallel to the film surface were performed to determine the Curie temperature T_C. Figure 1 shows the magnetization for annealed and as-deposited LCMO and LBMO films on different substrates. All samples show a clear ferromagnetic transition. The Curie temperature was defined by the maximum slope of the magnetization; Curie temperatures obtained in this way are given in Table I. The as-deposited LCMO films and the as-deposited LBMO films have a T_C of about 230 K and 300 K independent of the substrate material. Annealing in flowing oxygen for 2 h at 950 °C enhances the Curie temperature for LCMO and LBMO films to about 270 K and 313 K, respectively. These values agree with literature values for fully oxygenated LCMO and LBMO crystals at the doping level $x=0.3$.[15] Therefore we believe that our annealed films are fully oxygenated.

The resistivity of the samples is shown in Fig. 2. For both LCMO and LBMO films a characteristic pattern emerges. The epitaxial films on $LaAlO_3$ and $SrTiO_3$ show a sharp metal-insulator transition close to the ferromagnetic transition. Indeed, the temperatures T_r of maximum zero-field resistivity slope are very close to the Curie temperatures; see Table I. The films on Si and sample LBA1SR show a change from positive to negative resistivity slope as well. This transition, however, is broad and the temperature T_r is considerably lower than the Curie temperature. The annealed LCMO and LBMO films on $LaAlO_3$ have a small resistivity with 87 $\mu\Omega$ cm and 48 $\mu\Omega$ cm at 100 K, respectively. The resistivity of the as-deposited films is roughly one order of magnitude higher. However, the similar temperature dependence indicates that the resistivity of the as-deposited films is of intrinsic origin either. The resistivity of sample LBA1SR and of the films on Si is much larger and shows a different temperature dependence; it is determined by extrinsic properties, presumably grain boundary scattering. This interpretation is consistent with the temperature dependence of the measured magnetoresistance ratio

$$\Delta\rho/\rho_0=\frac{\rho(1\ \mathrm{T})-\rho(0\ \mathrm{T})}{\rho(0\ \mathrm{T})}. \tag{7}$$

Figure 3 shows that the magnetoresistance of epitaxial films on $LaAlO_3$ and $SrTiO_3$ has a maximum near the Curie temperature, whereas films on Si and sample LBA1SR show a large magnetoresistance at low temperatures.

B. The high-temperature resistivity

The resistivity data in the paramagnetic phase were fitted with the four models described in Sec. II, i.e., the polaron model in the adiabatic, Eq. (2), and nonadiabatic, Eq. (3), regime, the band-gap model, Eq. (1), and the variable-range hopping model, Eq. (5). The resistivity for the small polaron model in the adiabatic regime is $\rho=AT\exp(W_p/kT)$. The small polaron model in the nonadiabatic regime did not fit the data well and gave inconsistent results. The values of the electronic transfer integral t obtained from the measured re-

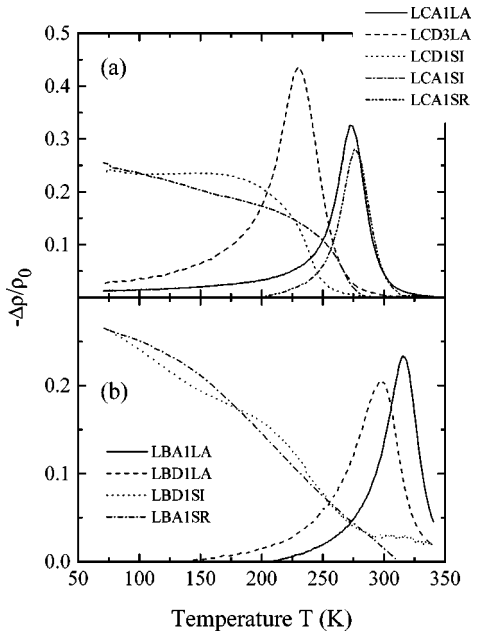

FIG. 3. Magnetoresistance ratio $\Delta\rho/\rho_0$ of various (a) LCMO and (b) LBMO films in a field of 1 T applied parallel to the film.

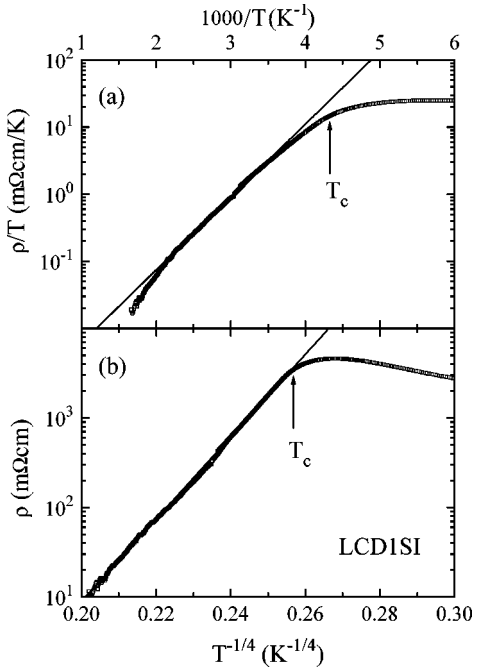

FIG. 4. (a) ρ/T shown as a function of inverse temperature (top axis) for the as-deposited $La_{0.7}Ca_{0.3}MnO_3$ film on Si. The polaron model, Eq. (2), fits the data in a limited temperature range above T_C (solid line), but clear deviations are apparent at high temperatures. (b) Resistivity of the same sample as a function of $T^{-1/4}$ (bottom axis). The solid line is a fit of the variable-range hopping model, Eq. (5), to the data.

sistivity with Eq. (3) were always larger than the limiting value $t_{\max}$ given by Eq. (4). The limiting value was estimated approximating the longitudinal optical phonon frequency by the Debye frequency $\omega_0 \sim k\Theta_D/\hbar$.

The band-gap model gave an acceptable description of the resistivity of the epitaxial films. However, the activation energies of the annealed films were small, $E_g/k \simeq 700$ K. For a conventional semiconductor metallic behavior is expected in the temperature range $kT > E_g/2$, where the fitting was actually done. Since this is not observed, we discard the band-gap and the mobility-edge models as unlikely. This conclusion is in agreement with the work of Wilson *et al.*:[16] In fully oxygenated LSMO films an Arrhenius law can be seen up to 600 K with an activation energy of only 210 K.

In the following we concentrate on the polaron model and the variable-range hopping model.

1. Films on Si

The data of the as-deposited $La_{0.7}Ca_{0.3}MnO_3$ film on Si, sample LCD1SI, are analyzed in Fig. 4. In Fig. 4(a) ρ/T is shown as a function of the inverse temperature. The solid line is a fit of the polaron model, Eq. (2). Though the model agrees with the data in a limited temperature range above T_C, deviations are clearly seen at higher temperatures. In Fig. 4(b) the resistivity ρ is shown as a function of $T^{-1/4}$. The solid line is a fit to the variable-range hopping model, Eq. (5); this fit remarkably agrees with the data in the measured temperature range above T_c, i.e., $230.5 < T < 600$ K. The data are clearly in favor of the variable-range hopping model. The annealed $La_{0.7}Ca_{0.3}MnO_3$ film on Si as well as the as-deposited $La_{0.7}Ba_{0.3}MnO_3$ film on Si show a similar behavior. The resistivity of those films can be fitted to the polaron model in a limited temperature range; deviations, however, are seen at higher temperatures. The variable-range hopping model describes the resistivity in the complete measured temperature range above T_c. The fitting parameters for the two models are presented in Table II.

2. Films on $LaAlO_3$ *and* $SrTiO_3$

The epitaxial films on $LaAlO_3$ and $SrTiO_3$ were analyzed in a similar way as the data on the polycrystalline films on Si. In Fig. 5(a) ρ/T is shown as a function of the inverse temperature for an as-deposited film on $LaAlO_3$. The solid line is a fit of the polaron model, Eq. (2), to the data. It gives a convincing fit above the Curie temperature. Clear deviations between the variable-range hopping model, Eq. (5), and the data are found; see Fig. 5(b). These results are typical for all investigated epitaxial films on $LaAlO_3$ and $SrTiO_3$.

The film LBA1SR, however, behaved differently. As already apparent from Fig. 2(b) the resistivity of this film is quite high and the transition is broad indicating a highly defective microstructure. The high-temperature resistivity is nicely fitted by the variable-range hopping model, Eq. (5), above 294 K, whereas the polaron model, Eq. (2), fits the data less well. This finding shows that variable-range hopping is not a peculiarity of films on Si but is a signature of films with a defective microstructure.

The fitting parameters are given in Table II.

C. Transition region

In this section we investigate the transition region, especially the relation between resistivity and magnetization near T_C and the dependence of the metal-insulator transition temperature T_r on the applied field.

We use the phenomenological expression

$$\rho = AT \exp\left[\frac{W_p(M)}{kT}\right] \tag{8}$$

TABLE II. Fitting parameters of the various samples for the polaron and the variable-range hopping (VRH) model. The values in brackets are only valid in a limited temperature range.

Sample	Polaron W_p (meV)	A (mΩ cm/K)	VRH T_0 (10^6 K)	ρ_∞ (mΩ cm)
LCA1SR	66	6.1×10^{-4}	(0.058	5.3×10^{-2})
LCA1LA	66	6.7×10^{-4}	(0.066	5.2×10^{-2})
LCD1LA	103	2.1×10^{-3}	(2.56	2.2×10^{-3})
LCD2LA	102	2.1×10^{-3}	(2.56	2.1×10^{-3})
LCD3LA	101	2.1×10^{-3}	(1.87	4.0×10^{-3})
LCA1SI	(181	2.6×10^{-3})	60.0	5.3×10^{-7}
LCD1SI	(215	5.0×10^{-4})	126.2	5.5×10^{-9}
LBA1LA	86	1.83×10^{-4}	(0.16	9.8×10^{-3})
LBD1LA	95	3.6×10^{-4}	(0.39	8.2×10^{-3})
LBD1SI	(237	1.3×10^{-4})	187.4	2.4×10^{-10}
LBA1SR	(164	5.5×10^{-4})	13.0	4.0×10^{-5}

to extract an effective activation energy from the data taken *below* T_c. The prefactor A determined from the analysis of the high-temperature resistivity is used in the calculation. Figure 6 shows the activation energies for the annealed LCMO films LCA1SR and LCA1LA as well as for the LBMO film LBA1LA as a function of the reduced magnetization M/M_0. M_0 is determined from the measured magnetization by extrapolation to zero temperature and is assumed to be a rough measure of the saturation magnetization. For all films we find a linear dependence of the activation energy on the magnetization for a considerable range of magnetization values. Deviations are seen at small magnetizations, probably due to sample inhomogeneities and fluctuation effects. The activation energy extrapolates to zero for magnetizations near the zero-temperature magnetization. The arrows in Fig. 6 indicate the activation energies obtained from the high-temperature resistivities. These values agree very well with the activation energies obtained from the extrapolation to zero magnetization. A similar exponential dependence of the resistivity on the magnetization was reported by Hundley *et al.*[17]

We have studied the dependence of the metal-insulator transition temperature T_r on the magnetic field in the annealed LBMO and LCMO films. Figure 7 shows the temperature shift of the metal-insulator transition as a function of the applied magnetic field for the films LBA1LA and LCA1LA. $T_r(H)$ was determined by a constant resistivity criterion set by the zero-field resistivity and the zero-field

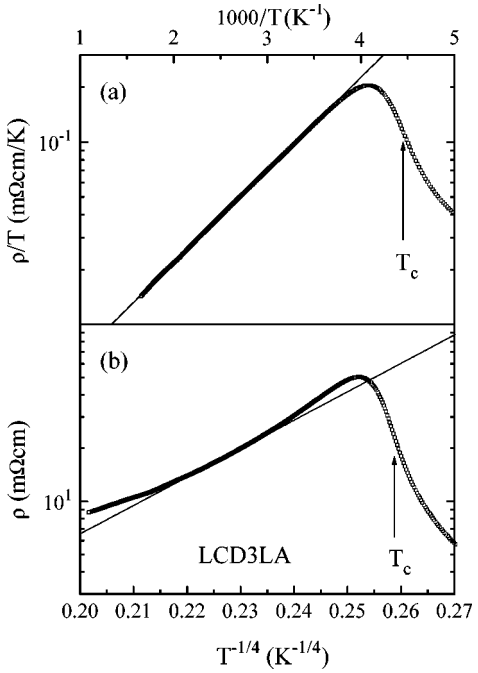

FIG. 5. (a) ρ/T of an as-deposited $La_{0.7}Ca_{0.3}MnO_3$ film on $LaAlO_3$ shown as a function of inverse temperature (top axis). The solid line is a fit of the polaron model, Eq. (2). (b) Resistivity of the same sample as a function of $T^{-1/4}$ (bottom axis). The solid line is a fit of the variable-range hopping model, Eq. (5), to the data.

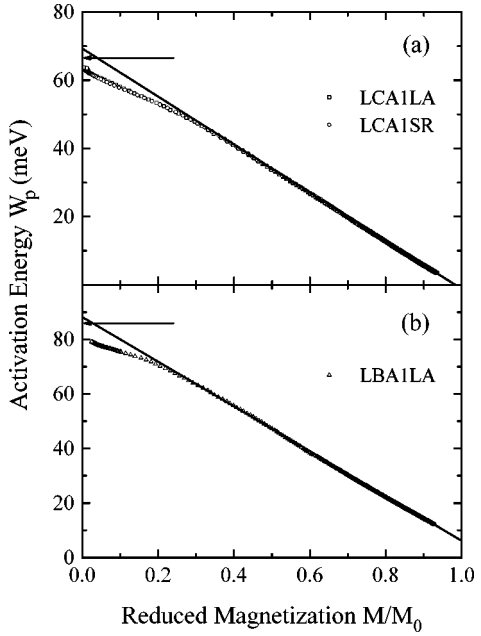

FIG. 6. Activation energies in the ferromagnetic phase as a function of the reduced magnetization M/M_0 for (a) the LCMO films LCA1LA and LCA1SR and (b) the LBMO film LBA1LA. The activation energies were calculated with Eq. (8) from the measured zero-field resistivity. The magnetization was measured in magnetic fields of 0.1 T.

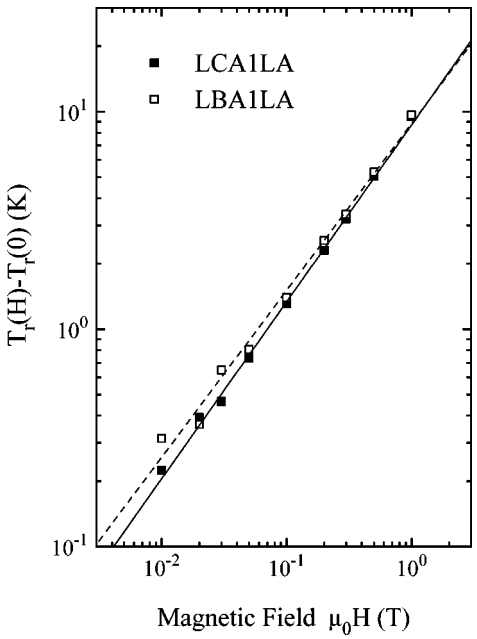

FIG. 7. Shift of the metal-insulator transition temperature T_r as a function of the applied field. The solid and dashed lines show fits of the power law, Eq. (9), to the data for samples LCA1LA and LBA1LA, respectively.

transition temperature derived from magnetization. The metal-insulator transition temperature shifts with the applied field according to a power law. We find

$$T_r(H)-T_r(0)=T_r(0)(H/H_0)^s \tag{9}$$

with $s=0.77\pm0.03$, $\mu_0 H_0=105.3$ T for sample LBA1LA and $s=0.81\pm0.02$, $\mu_0 H_0=69.4$ T for sample LCA1LA, respectively.

V. DISCUSSION AND CONCLUSIONS

A. Polycrystalline films

Our data on polycrystalline LCMO and LBMO films are remarkably well fitted by the variable-range hopping model in the temperature range $T_C<T<600$ K. Using the density of states $N(E_F)=2.4\times10^{28}$/eV m^3 determined from specific-heat measurements on $La_{0.7}Sr_{0.3}MnO_3$ (Ref. 18) we derive localization lengths $\xi\sim0.3$ Å for our films on Si and $\xi\sim0.7$ Å for sample LBA1SR. Viret *et al.*[3] found similar values. Since the localization length is expected to be of the order of the Mn-Mn separation, these values are unphysical. However, the comparison with the epitaxial films shows that the variable-range hopping behavior is extrinsic, i.e., is related to nonstoichiometric regions or to tunneling processes across grain boundaries. It is therefore hard to justify the use of the intrinsic density of states in the calculation of the correlation length. It is much more likely that the resistivity is determined by sample regions with a much lower carrier density. This is in agreement with the fact that the samples on Si show a much higher overall resistivity than the epitaxial films.

B. Epitaxial films

The results clearly show that the resistivity of epitaxial manganite films in the paramagnetic regime is best described by the polaron model in the adiabatic limit. The ordinary Hall effect near T_C is found to be holelike with $R_H=0.06\pm0.01$ $\mu\Omega$ cm/T for both LCMO and LBMO films.[19] In a one-band model this corresponds to a carrier density of 0.6 holes/unit cell in rough agreement with the doping level. From the measured resistivity and Hall effect we can deduce mobilities for the annealed LCMO and LBMO films of about 0.3 cm^2/V s and 0.7 cm^2/V s, respectively. In a free-electron model mean free paths of 1.4 Å and 3.0 Å are calculated for the LCMO and the LBMO film near T_C. These small mean free paths are not consistent with band transport.

From the measured resistivity the value of the longitudinal optical-phonon frequency ω_0 can be estimated with Eq. (2). We use a hopping distance $a\simeq7$ Å derived under the assumption that the carrier density is given by the chemical doping and that all carriers form polarons. We obtain $\omega_0=2\times10^{13}$ Hz and 6×10^{12} Hz for the annealed and as-deposited LCMO films, and $\omega_0=7\times10^{13}$ Hz and 4×10^{13} Hz for the annealed and as-deposited LBMO films, respectively. The values for the LCMO films are somewhat higher than the values of the transverse optical-phonon frequencies for the Mn-O bending and stretching modes that have been measured in polycrystalline LCMO samples.[20] The hopping energy W_p is found to be about 0.1 eV. In the adiabatic limit the polaron formation energy is $E_p=2(W_p+t)\sim1.4$ eV with a transfer integral $t\sim0.6$ eV.[9] A polaron radius r_p can be defined for a small polaron in an ionic crystal.[13] From the measured value $E_p\sim1.4$ eV we obtain $r_p\sim5$ Å. This value is in reasonable agreement with the unit-cell parameter of 3.88 Å.

The polaron scenario is especially appealing, since it is in agreement with thermopower[12,21,22] and Hall resistivity[23] measurements. The thermopower of the manganites is found to be activated above T_C. The activation energy derived from thermopower data is considerably smaller than the activation energy derived from resistivity, which is a characteristic of small polarons. Jaime *et al.*[23] observed a thermally activated Hall resistivity in $(La_{(1-x)}Gd_x)_{0.67}Ca_{0.33}MnO_3$ films with an activation energy equal to 2/3 of the resistivity activation energy. This result is expected for the hopping of small polarons on a triangular lattice.

According to the results of Röder *et al.*[10] the small polarons are dressed with a spin cloud. Since the metal-insulator transition is magnetically driven, it is likely that the developing ferromagnetism strongly enhances the mobility, i.e., reduces the polaron hopping energy W_p. Millis *et al.*[9] find that the hopping integral t is enhanced by the magnetic ordering, leading in mean-field theory to an effective hopping matrix element $t[(1+(M/M_S)^2)/2]^{1/2}$. M_S denotes the saturation magnetization. According to Eq. (2) this leads to a decrease in the polaron hopping energy. Experimentally we find a linear magnetization dependence of the effective polaron hopping energy that is much stronger than the mean-field prediction.

The electrical transport properties of the manganites are similar to the situation found in doped EuO. A metal-insulator transition coinciding with a ferromagnetic transi-

tion has been found in europium-rich EuO.[24] Penney *et al.*[25] report the observation of a thermally activated resistivity above the transition and of a large magnetoresistance near the ferromagnetic transition. The activation energy is found to decrease linearly in the ferromagnetic region.[25] Various models have been proposed to understand the behavior in EuO.[25,26] Especially the model of Emin *et al.*[26] might have some relevance in understanding the metal-insulator transition in the manganites. Emin *et al.*[26] study magnetopolaron effects as a function of the ferromagnetic order in a continuum approximation; their model is very similar to the model of Röder *et al.*[10] Emin *et al.*[26] find that the transition is due to the abrupt collapse of delocalized carriers into small polarons that is triggered by the loss of ferromagnetic long-range order. In this case the contribution of spin distortions to the localization of small polarons is important, since lattice distortions alone cannot trap the small polarons. In EuO, however, conduction occurs via motion in impurity bands. Emin *et al.*[26] calculated that the temperature of the small polaron collapse depends on the square root of the applied field; this result might strongly depend on the specific model assumptions, especially the spin-wave spectrum.

For the manganites a similar scenario seems possible. If the electron-transfer energy and the electron-phonon coupling energy are nearly equal, spin disorder plays a decisive role in determining whether the carriers are severely localized or extended. Thus the onset of ferromagnetic order leads to an abrupt expansion of the polaron radius, leading to the formation of bands and metallic conductivity. Experimentally we find a sublinear dependence of the metal-insulator transition temperature T_r on the applied field. The scaling exponent, however, is about 0.8.

In conclusion, we found that the resistivity of epitaxial manganite thin films shows distinctive effects of small polaron motion. In the ferromagnetic phase the polaron hopping energy decreases linearly with the magnetization. The metal-insulator transition temperature depends sublinearly on the applied magnetic field. Both features are in qualitative agreement with the models of Röder *et al.*[10] and Emin *et al.*[26] for the abrupt collapse of extended states to localized small polaronic states triggered by the loss of ferromagnetic order.

ACKNOWLEDGMENTS

This work was supported by the European Union TMR ''OXSEN'' network. We thank Simon Sena for providing the samples LCD1LA and LCD2LA.

[1] J. M. D. Coey, M. Viret, and S. von Molnar, Adv. Phys. (to be published).
[2] R. M. Kusters, J. Singleton, and D. A. Keen, Physica B **155**, 362 (1989).
[3] M. Viret, L. Ranno, and J. M. D. Coey, Phys. Rev. B **55**, 8067 (1997).
[4] G. J. Snyder, R. Hiskes, S. DiCarolis, M. R. Beasley, and T. H. Geballe, Phys. Rev. B **53**, 14 434 (1996).
[5] C. Zener, Phys. Rev. **82**, 403 (1951).
[6] P.-G. de Gennes, Phys. Rev. **118**, 141 (1960).
[7] C. W. Searle and S. T. Wang, Can. J. Phys. **48**, 2023 (1970).
[8] K. Kubo and N. Ohata, J. Phys. Soc. Jpn. **33**, 21 (1972).
[9] A. J. Millis, B. I. Shraiman, and R. Mueller, Phys. Rev. Lett. **77**, 175 (1996); A. J. Millis, R. Mueller, and B. I. Shraiman, Phys. Rev. B **54**, 5405 (1996).
[10] H. Röder, J. Zang, and A. R. Bishop, Phys. Rev. Lett. **76**, 1356 (1996); J. Zang, A. R. Bishop, and H. Röder, Phys. Rev. B **53**, R8840 (1996).
[11] J. M. D. Coey, M. Viret, L. Ranno, and K. Ounadjela, Phys. Rev. Lett. **75**, 3910 (1995).
[12] M. Jaime, M. B. Salamon, M. Rubinstein, R. E. Treece, J. S. Horwitz, and D. B. Chrisey, Phys. Rev. B **54**, 11 914 (1996).
[13] Sir Nevill Mott, *Conduction in Non-Crystalline Materials* (Clarendon Press, Oxford, 1993), p. 17ff.
[14] L. J. van der Pauw, Philips Tech. Rev. **20**, 220 (1958).
[15] A. P. Ramirez, J. Phys.: Condens. Matter **9**, 8171 (1997).
[16] M. L. Wilson, J. M. Byers, P. C. Dorsey, J. S. Horwitz, D. B. Chrisey, and M. S. Osofsky, J. Appl. Phys. **81**, 4971 (1997).
[17] M. F. Hundley, M. Hawley, R. H. Heffner, Q. X. Jia, J. J. Neumeier, J. Tesmer, J. D. Thompson, and X. D. Wu, Appl. Phys. Lett. **67**, 860 (1995).
[18] B. F. Woodfield, M. L. Wilson, and J. M. Byers, Phys. Rev. Lett. **78**, 3201 (1997).
[19] M. Ziese and C. Srinitiwarawong (unpublished).
[20] K. H. Kim, J. Y. Gu, H. S. Choi, G. W. Park, and T. W. Noh, Phys. Rev. Lett. **77**, 1877 (1996).
[21] M. Jaime, M. B. Salamon, K. Pettit, M. Rubinstein, R. E. Treece, J. S. Horwitz, and D. B. Chrisey, Appl. Phys. Lett. **68**, 1576 (1996).
[22] T. T. M. Palstra, A. P. Ramirez, S-W. Cheong, B. R. Zegarski, P. Schiffer, and J. Zaanen, Phys. Rev. B **56**, 5104 (1997).
[23] M. Jaime, H. T. Hardner, M. B. Salamon, M. Rubinstein, P. Dorsey, and D. Emin, Phys. Rev. Lett. **78**, 951 (1997); J. Appl. Phys. **81**, 4958 (1997).
[24] M. R. Oliver, J. A. Kafalas, J. O. Dimmock, and T. B. Reed, Phys. Rev. Lett. **24**, 1064 (1970).
[25] T. Penney, M. W. Shafer, and J. B. Torrance, Phys. Rev. B **5**, 3669 (1972).
[26] D. Emin, M. S. Hillery, and N. L. Liu, Phys. Rev. B **35**, 641 (1987); M. S. Hillery, D. Emin, and N. L. Liu, *ibid.* **38**, 9771 (1988).